Modeling and characterization of OASIS inflatable primary antenna by dual modality metrology

SIDDHARTHA SIRSI,[1,2,*] HENRY QUACH,[2] HYUKMO KANG,[2] PETE MORKEN,[3] ARTHUR PALISOC,[4] YUZURU TAKASHIMA,[2] CHRISTIAN D'AUBIGNY,[5] AMAN CHANDRA,[1] MARCOS ESPARZA,[2] KARLENE KARRFALT,[2] KEVIN Z. DERBY,[2] HEEJOO CHOI,[2,6] DAEWOOK KIM,[1,2,6,7] AND CHRISTOPHER WALKER[1,2,8]

[1]*Department of Astronomy and Steward Observatory, University of Arizona, 933 N. Cherry Ave., Tucson, AZ 85721, USA*
[2]*Wyant College of Optical Sciences, University of Arizona, 1630 E. University Blvd., Tucson, AZ 85721, USA*
[3]*Nikon Metrology, Inc., Brighton, MI 48116, USA*
[4]*L'Garde, Inc., 15181 Woodlawn Avenue, Tustin, CA 92780, USA*
[5]*Raytheon, Tucson, AZ, USA*
[6]*Large Binocular Telescope Observatory, University of Arizona, 933 N. Cherry Ave., Tucson, AZ 85721, USA*
[7]*dkim@optics.arizona.edu*
[8]*cwalker@arizona.edu*
[*]*siddharta.sirsi@gmail.com*

Abstract: OASIS (Orbiting Astronomical Satellite for Investigating Stellar Systems) is a space-based observatory with a 14 m diameter inflatable primary antenna that will perform high spectral resolution observations at terahertz frequencies. The large inflatable aperture, non-traditional surface configuration, and the double layered membrane structure afford unique challenges to the modeling and testing of the primary antenna. A 1-meter prototype of the primary antenna (A1) was built to validate our technical approach. A laser radar coordinate measuring system was adopted to measure the shape of A1. In addition, deflectometry was performed to monitor the stability of A1 during the radar measurement. Test cases pertaining to specific operational conditions expected for the 14 m OASIS primary were explored. The measured data were then compared to the Fichter model and Finite-element Analyzer for Inflatable Membranes (FAIM).

1. Introduction

OASIS (Orbiting Astronomical Satellite for Investigating Stellar Systems) is a proposed space-based infrared observatory (63 - 660 μm) which will provide key insights into the role water plays in the evolution of stars, planetary systems, and galaxies [1]. For the science requirement of observation sensitivity, OASIS employs a 14-meter diameter inflatable membrane primary reflective antenna (A1) as shown in Fig. 1. Utilizing a traditional optics fabrication approach, the cost of realizing a 14-meter class primary would likely be viewed as prohibitive. We proposed a large inflatable optics that could be collapsed to a small volume, thereby dramatically lowering cost, and maximizing the photon collecting efficiency per dollar. A1 consists of two membranes, a front canopy, and a back reflector, that are sandwiched together around their circumference with flanges. Gas is injected between the membranes to realize a lenticular structure (see Fig. 2). The front canopy can be either black Kapton or transparent Kapton. Both are transparent over the wavelength range OASIS will operate. Black Kapton has the added advantage of blocking

visible wavelengths. The back reflector membrane is made out of a 12.7 μm (i.e., 0.5 mil) thick aluminized Mylar or Kapton. Mylar and Kapton are suitable candidates for space environment application due to their low outgassing, resistance to radiation weathering, and temperature stability [2].

Fig. 1. OASIS Mission concept showing the 14 m diameter deployed inflatable membrane antenna (A1) configuration on the right side while the corrector optics and detectors are located inside the payload structure on the left.
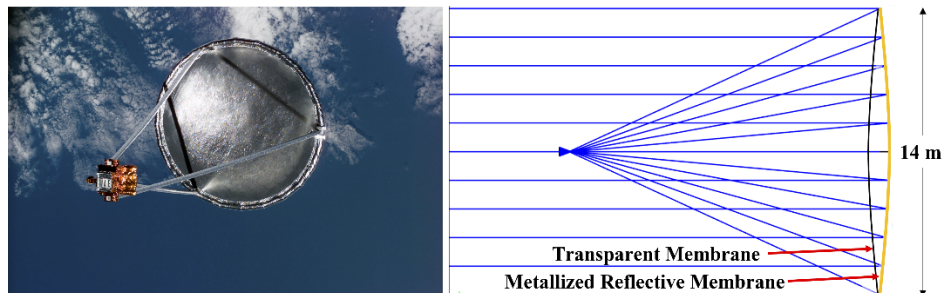
Fig. 2. (Left) Inflatable Aperture Experiment (IAE) demonstrated a 14 m inflatable aperture in space (1996). (Right) Ray trace of 14 m diameter A1 of OASIS showing the incoming signal passing through the clear membrane and focused by the concave metallized membrane [3].

The first mathematical description of mirrors formed utilizing this architecture was provided by Hencky [4]. Fichter [5] re-examined Hencky's original analysis and corrected an algebraic error along with retaining more terms to assess convergence. Moreover, L'Garde Inc has developed a Finite Element Analyzer for Inflatable Membranes (FAIM) code for determining the stresses and deformations of inflatable shell membranes under specific internal pressure condition [6].

In this paper, we model and measure a 1-meter prototype membrane mirror in order to check the fidelity of our surface modeling and testing solutions. Because the unit under test (UUT) is not a rigid optical surface with a traditional spherical (or parabolic) shape, conventional optical testing such as interferometer and contact-type profilometer could not be performed due to the

required dynamic range and compressibility of testing surfaces. An Accurate Precision Distance Scanning lidar system (APDIS MV430, Nikon) was used to measure absolute surface profile to provide the comprehensive optical surface metrology. Deflectometry utilizing the non-null optical testing method was used to monitor the stability of surfaces during the lidar measurements.

In Section 2, the three inflatable optics prediction models are presented with key simulation parameters. The test setup and testing parameters are presented in Section 3. We elucidate the measurement results of deflectometry and radar along with the modeled surface shape in Section 4.

2. Modeling of inflated membrane

An inflatable mirror of the type described above will produce a surface that is neither spherical nor parabolic, but an oblate spheroid called Hencky curve [4,7]. Hencky's solution neglects the radial component of pressure acting on the deformed membrane. Fichter [5] revised Hencky's original solution to include the radial component of applied pressure. He also corrected an algebraic error and retained more terms to assess convergence. The dimensionless lateral deflection is then given by

$$W(\rho) = q^{2/3} \sum_{0}^{\infty} a_{2n}(1 - \rho^{2n+2}),$$ (1)

where W is the dimensionless lateral deflection, $q = pa/Eh$ is the dimensionless loading parameter, p is the pressure, a is the radius of the membrane, E is the modulus of elasticity, h is the thickness of membrane, a_{2n} are the coefficients in power series, and ρ is the dimensionless radial coordinate. The complete description of the coefficients of the power series are reported in [5]. This analytical solution is used as the benchmark method to model and calculate the surface profile of the 1-meter prototype based on the parameters listed in Table 1.

Table 1. Analytical inflatable optics modeling parameters

Parameter	
Membrane Material	Mylar
Thickness	51 μm (i.e., 2 mil)
Poisson's Ratio	0.38
Elastic Modulus	0.73×10^6 psi
Diameter	1 m
Pressure	480 to 520 Pa

FAIM (Finite-element Analyzer for Inflatable Membranes) is a geometric nonlinear general-purpose finite element code for determining the stresses and deformations of inflatable shell membranes due to internal pressure, nodal forces, and temperature loads [6]. It uses a numerically intensive, iterative procedure to solve the nonlinear equilibrium equations to a user-specified desired degree of accuracy. The stiffness and mass matrix generated by the code may be input to an eigenvalue solver to calculate modes and natural frequencies. FAIM employs a 6-node isoparametric triangle, an 8-node isoparametric quadrilateral, a 3-node tension only cable element, and a 2-node space frame element (Fig. 3 left) to model the deformation of monolithic membranes as well as gored membranes which are stitched together. Although a 3-node triangle and a 4-node quadrilateral provides computational advantage, they are not adequate to determine the surface slope throughout the continuum. The 3-node tension only cable element is used to model the effect of stiffer, thicker seams in the case of gored membranes.
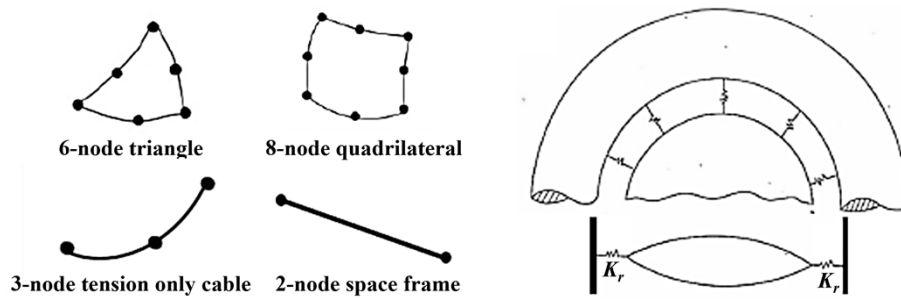
Fig. 3. (left) Elements in the FAIM Library. (right) The toroidal support ring is replaced by springs with spring constant K_r [6].

A spring boundary condition is used to characterize the mount or outer tensioning ring. The toroidal ring supporting structure is replaced by springs (Fig. 3 right) with a spring constant

$$K_r = \frac{EA}{R^2}, \tag{2}$$

where E is the torus material modulus, A is the cross-sectional area of the torus, and R is the major torus radius. This numerical modeling tool is effective in realizing 10 to 20 m scale precision inflatable space optical surfaces, such as OASIS, with minimal wavefront aberrations.

3. Inflatable antenna metrology

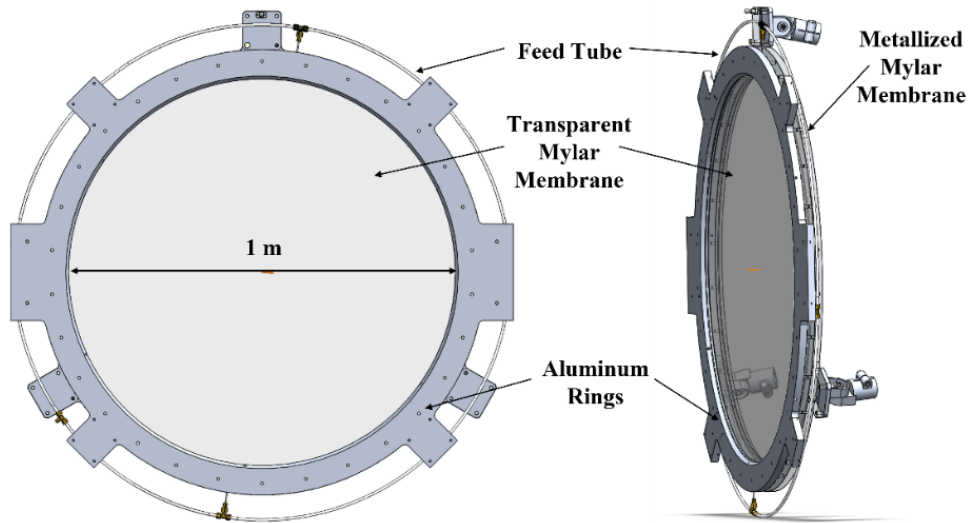### 3.1. Sub-scale 1-meter inflatable optic prototype

A sub-scale 1 m prototype of A1 was designed, modeled, and optimized using FAIM. The optimized inflatable membrane prototype was manufactured and assembled to be measured and compared against the predicted surface profile. The prototype consists of 51 μm (i.e., 2 mil) thick transparent and metallized mylar membranes sandwiched between three aluminum flanges as shown in Fig. 4. The sealed membrane is pressurized with nitrogen gas using a pressure control unit developed in-house with a resolution of +/-5 Pa.

By pressurizing the sealed membrane, a convex transparent surface and a concave metallized surface are inflated and formed with the predicted target surface profiles. The incoming signal passes through the front transparent layer and gets reflected off the primary mirror (metallized mylar) surface. In the OASIS implementation, the reflected light comes to a focus inside an optics module that corrects for aberrations before being detected.
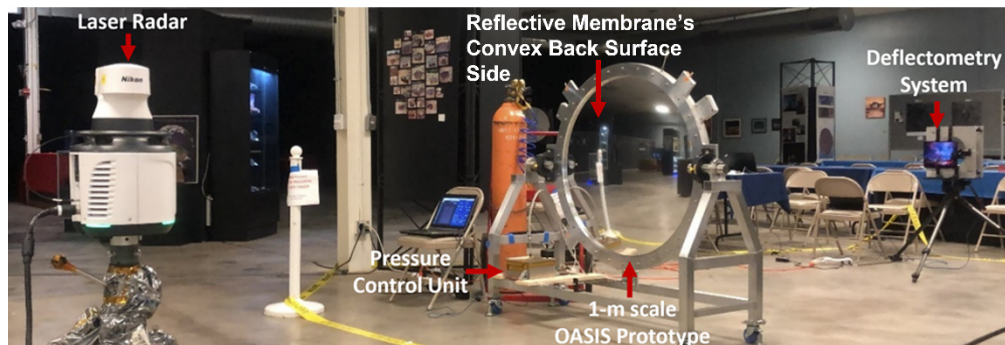
3.2. Verification metrology using laser radar and deflectometry

The Nikon APDIS is a laser radar metrology instrument (i.e., lidar) capable of high precision, non-contact surface measurements for a UUT having large area. It utilizes a spherical coordinate system measurement technology where a point in 3-D space is determined by two angles and a range. The elevation and azimuthal angles are measured with high precision rotary encoders. The range is measured with a collimated infrared laser heterodyne interferometer. The system is capable of ~10 ppm, 3-dimensional accuracy over 30- or 50-meter distances. For our test setup shown in Fig. 5, at 2 meters away from the test unit, the expected accuracy of the 3-dimentional coordinate is ~28 μm (i.e., ~0.001 inch). Higher profile measuring accuracy is possible, if the line-of-sight is aligned such that it favors using ranging versus angle measuring. Table 2 shows the nominal accuracy and dynamic ranges of APDIS MV430 [8].

A deflectometry system (right side in Fig. 5) was used in parallel with the lidar system to monitor temporal variations of the surface shape. Deflectometry is an incoherent surface

Fig. 4. Sub-scale 1-meter inflatable primary antenna (A1) prototype consisting of 51 μm (i.e., 2 mil) thick transparent and metallized mylar membranes sandwiched between three aluminum flanges.

Fig. 5. (a) Verification metrology test setup: 1-m OASIS A1 prototype, Nikon APDIS Laser Radar, and Deflectometry system. The APDIS is measuring the reflective membrane's convex back surface (i.e., back side of A1) directly. The deflectometry system (the display and camera unit on the right side of the photo) is measuring the same A1 reflective membrane surface from the front side through the transparent canopy surface. (Note: The transparent mylar membrane is facing the deflectometry system and is not visible from this view angle.) This is a simultaneous cross-checking metrology setup [8].

Table 2. Maximum possible error (MPE) of Nikon APDIS MV430.

	Range	Azimuth	Elevation
Working Limit	0.5 m – 30 m	± 180°	±45°
Accuracy (MPE)	20 μm + 5μm/m	13.6 μm/m	

metrology technique that does not require nulling conditions. Leveraging the reverse Hartman test principal, the deflectometry method can measure the slope distribution of the UUT with high spatial resolution within 20 sec.

During a deflectometry measurement, a pattern-and-modulated illumination source (e.g., computer monitor) illuminates the surface of the UUT. A camera records the reflected patterns and ray tracing is used to determine the local slopes of the cross-section where the ray hits. Deflectometry's strengths are its sensitivity and large dynamic slope-measuring range. However, it requires careful position calibration for low order shape testing. Thanks to the flexibility and sensitivity of the deflectometry technique, we were able to measure the shape of the 1-meter A1 prototype while it underwent testing in a thermal vacuum chamber [9].

The terminology used for describing the test set-up conditions for various verification test cases is illustrated in Fig. 6. In order to ascertain the feasibility of using APDIS for measuring the surface profile of primary antenna of OASIS, the following test cases are considered: Case 1) Measurement of the reflective surface through the transparent membrane as shown in Fig. 6 (left side), Case 2) Direct measurement of the convex reflective surface as shown in Fig. 6 (right side), Case 3) Accuracy loss at a measurement distance of 10 m compared to ~2 m under best possible conditions, and Case 4) High fidelity measurements when the return signal power is significantly diminished due to an increased angle of incidence of laser radar beam.
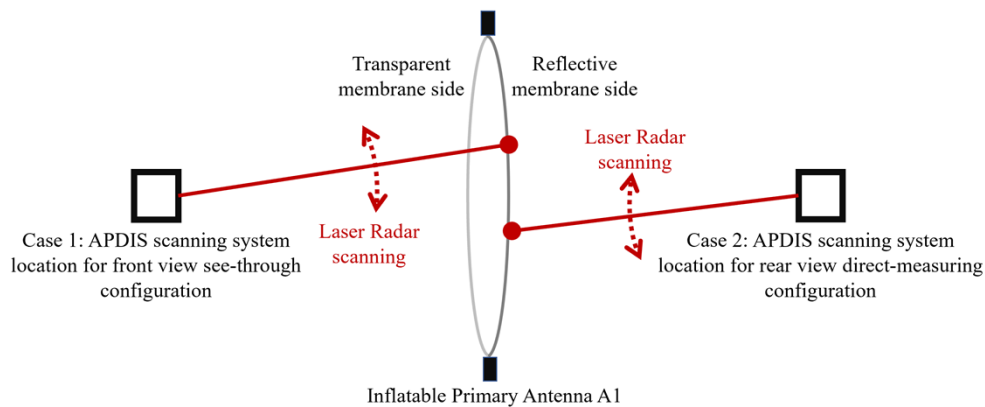
Fig. 6. (left side) APDIS is placed in front of A1 (i.e., Case 1: front view see-through configuration): Measurement of the concave surface is done through the transparent membrane. (right side) APDIS is placed behind A1 (i.e., Case 2: rear view direct-measuring configuration): Direct measurement of the convex reflective surface.

4. Metrology-based inflatable optics accuracy verification

4.1. A1 stability verification during the laser radar measurements

Given that the resolution of the pressure control unit is +/- 5 Pa and the maximum possible measurement error of APDIS is 28 μm from a distance of 2 m, the contribution of these two factors in producing repeatable accurate measurements must be considered. The back surface of A1 was measured twice at a constant pressure. The RMS drift in location between measurements was 0.43 μm, the RMS sag difference was 7.5 μm, and the peak-to-valley (PV) error between measurements was 22.5 μm. To determine the long-term stability of A1, measurements were taken on two separate days under the same conditions. The RMS sag difference between measurements was 46.28 μm and the PV error between measurements was 93.4 μm.

As stated earlier, in this verification context, deflectometry was used to monitor the stability of A1 over the duration of radar measurements. A typical radar line profile measurement takes

about 2 minutes for 240 points acquisition. Meanwhile, three deflectometry measurements were made over 2 min and each measurement is compared with the average of the 3 measurements to evaluate the RMS (Root Mean Square) deviation of surface profile. Figure 7 shows one series of subtracted surface maps. The RMS deviation of the surface profile over 2 minutes was ~160 nm. This is well below the sensitivity threshold of APDIS (~28 µm) and the A1 surface can be assumed to be static over the duration of radar measurement.
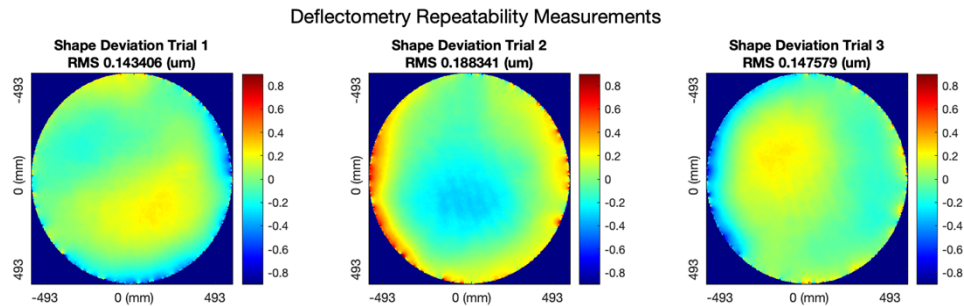

Fig. 7. From the deflectometry repeatability measurements the median surface changes between trials remains less than 200 nm, while the aperture edges possess the extrema representing the surface PV. The edges of an inflatable optic are susceptible not only to higher slopes, but also wrinkles.

From the deflectometry measurements it is clear that A1 is stable over the duration of the laser radar measurements (i.e., ~2 min). Due to the resolution of the pressure control unit, however, measurement errors larger than the APDIS maximum possible error can be induced over a longer time span.

4.2.   Agreement between bi-directional laser radar measurements

APDIS was placed 2.2 m in front (Case 1) and behind (Case 2) of A1 at an elevation of 1.3 m from ground. Four line profile measurements shown in Fig. 8 (left) with 240 points each were performed. A1 was inflated to a differential pressure of 500 Pa. APDIS was able to get a strong return signal, ~60 dB above the noise floor. The data is then fit to an 8th order polynomial and these polynomial coefficients are used to analyze the A1 surface by comparing different line profiles as shown in Fig. 8 (middle). The plots show the radial sag with the best fit sphere removed and represents the deviation of the measured surface from the ideal spherical surface design value, which was modeled and predicted by FAIM. The ideal membrane surface profile can be re-optimized for various other aspheric profiles depending on the final telescope optical design.

The RMS sag difference between Line 1 and Line 3 of plot shown in Fig. 8 (middle) is ~0.14 mm, and Line 2 and Line 4 is ~0.42 mm. This shows that A1 profile is not axially symmetric about the optical axis. This could be due to the uneven loading of the membrane, different elastic modulus values for mylar along transverse direction and machine direction, gravitational impact on flanges, or a combination of above. Both Case 1 and Case 2 confirm the anisotropic surface shape of A1 as the difference between front and back measurements are shown in Fig. 8 (right) with RMS average (four lines) value of 46 µm. The RMS of the difference profile is almost similar level of the mylar thickness (50.8 µm). This demonstrates that the reflective surface of inflatable membrane can be measured in both directions with high fidelity. This is an important confirmation as the measuring direction might be limited in various practical and logistical reason for a very large scale (e.g., 20 m in diameter) inflatable antenna metrology application. Based on this outcome, the rest of the measurements are carried out by placing APDIS behind A1 (i.e., Case 2 in Fig. 6).
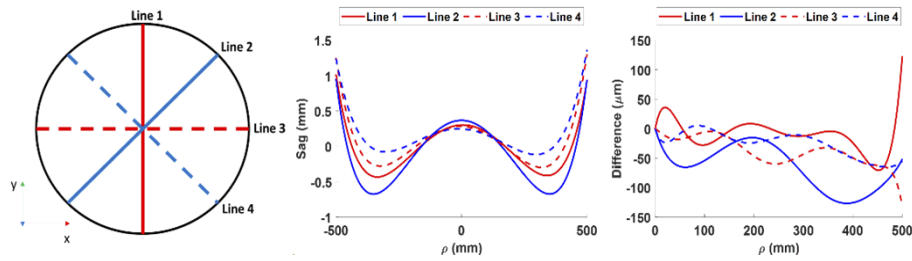
Fig. 8. (left) Different line profile measurements performed using APDIS. (middle) Plot of radial (ρ) sag with the best fit sphere removed while placing APDIS behind A1 and the convex reflective surface is directly measured. (right) Comparison between the Case 1 and Case 2 measurements defined in Fig. 5.

4.3. Laser radar accuracy verification under extreme conditions

APDIS was placed 10 m behind A1 (i.e., Case 3). All other conditions are identical to Case 2 and the same data acquisition-and-processing are implemented. Reflected signal dropped below detectable level around the periphery of the membrane due to large angle of incidence of the scanning beam. Measurable range on the membrane surface was truncated from ±500 mm to ±350 mm. The average of the difference RMS between all the line profiles of Case 2 and Case 3 is ∼9 μm as plotted in Fig. 9 (left). This demonstrates a superb accuracy performance compared to a typical error of 108 μm [8].

APDIS was placed behind A1 at around 53 deg off-axis location in the azimuthal direction as shown in Fig. 9 (top) with respect to the optical axis of A1 and at a distance of 2 m (Case 4). In this extreme incidence angle configuration, the APDIS was able to detect the reflected signal over up to ±330 mm from the center of the reflector. APDIS was unable to make reliable Line 4 measurements depicted in Fig. 8 (left) due to the loss of reflected signal. The average RMS error between Case 4 and Case 2 measurements is ∼38 μm as presented in Fig. 9 (right) which is comfortably within the maximum permissible error of 57 μm [8].

4.4. Numerical modeling accuracy of inflatable optics via FAIM

After testing and confirming the reliability of the laser radar in various configurations in Section 4.1, 4.2, and 4.3, the measurement data is compared with the Fichter model and FAIM predictions. The surface profile at a given pressure is modeled using the parameters listed in Table 1.

The reference data is measured at 2.2 m behind A1. The vertical (Line 1) and horizontal (Line 3) profile measurements with higher sampling (∼850 points) at pressure values ranging from 480 Pa to 520 Pa in steps of 10 Pa were made while monitoring and confirming the surface stability via deflectometry as verified in Section 4.1. The A1 shape differences for every 10 Pa steps are presented in Fig. 10 (left) and (middle). The overall surface sag profile changes match the analytical and numerical predictions for both vertical and horizontal profiles.

The radius of curvature (RoC) and sag of predicted models and measured data are compared in Table 3. Laser radar measurements are in close accordance with the Fichter model and FAIM predictions. Table 3 shows that both the models are in excellent agreement with a negligible 0.5% discrepancy confirming the essential numerical modeling capability of precision inflatable membrane optics via FAIM.

In practical operation of inflatable optics, the residual difference in RoC between FAIM and measured cases is compensated with defocus adjustments (e.g., focal plane shift) and/or by fine tuning the inflation pressure control. The slopes in Fig. 10 (right) represents RoC's sensitivity to pressure (i.e., *dRoC/dP*) and both models and the measured data slopes show similar tendency. The two term power series fit results of three lines are 2.47 mm/Pa, 2.48 mm/Pa and 2.63 mm/Pa
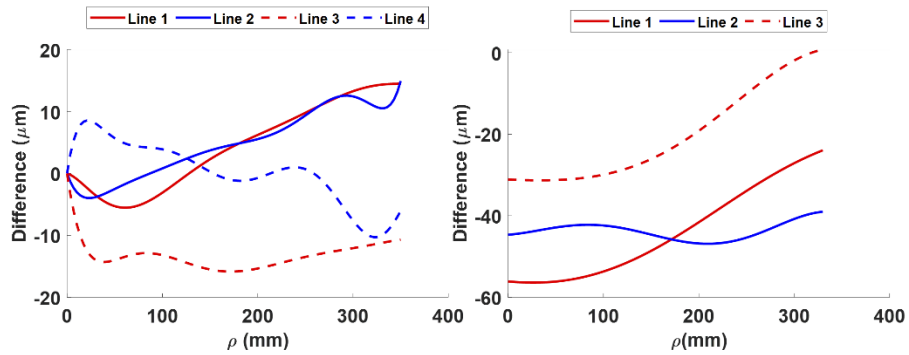
Fig. 9. (Top) Case 4: APDIS is placed at 53 deg off-axis position. (Bottom left) Radial profile (ρ) comparison between the 2 m (i.e., Case 2) and 10 m (i.e., Case 3) laser radar canning distance cases. (Bottom Right) Radial profile (ρ) comparison between the Case 2 and Case 4 measurements. (Note: Line numbers are defined in Fig. 7 (left).)
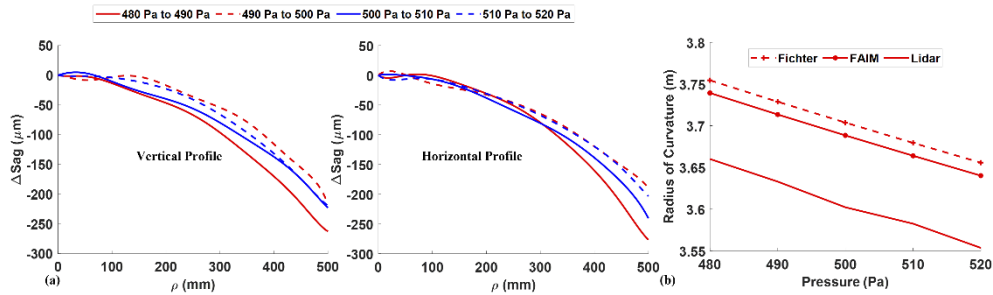
Fig. 10. (Left and middle) Measured sag profiles in vertical and horizontal directions at different pressures. Pressure is varied from 480 to 520 Pa in steps of 10 Pa. (right) Comparison of radius of curvatures between Fichter and FAIM models against the actual APDIS radar measurements at different pressures.

Table 3. Comparison between Fichter, FAIM, and APDIS laser radar measurement.

Pressure (Pa)	Radius of Curvature (m)			Sag (µm)				
	Model		Data	Model (PV)		Data (PV)	Δ Sag RMS	
	Fichter	FAIM	APDIS	Fichter	FAIM	APDIS	Fichter - APDIS	FAIM - APDIS
480	3.7545	3.7393	3.6601	30,965	30,964	31,769	403	422
490	3.7288	3.7135	3.633	31,179	31,178	32,032	426	445
500	3.7038	3.6884	3.6022	31,390	31,389	32,248	418	438
510	3.6794	3.664	3.5825	31,597	31,597	32,471	428	448
520	3.6557	3.6401	3.5535	31,803	31,802	32,690	425	446

for Fichter, FAIM, and laser radar data, respectively. They are matched with 6.5% difference that can be calibrated out for as-manufactured inflatable optics during the testing, integration, and assembly.

The relative RMS deviation of surface profile induced by 10 Pa change in pressure over the range of 480 to 520 Pa for Fichter, FAIM, and APDIS laser radar measurements are listed in Table 4. The rate of change of RMS deviation of surface profile with respect to pressure (i.e., $d(Dev)_{rms}/dP$) for Fichter model is 9.06 µm/Pa, 9.15 µm/Pa for FAIM, and 9.83 µm/Pa for the laser radar measurement. These characterization of A1 in terms of both $dRoC/dP$ and $d(Dev)_{rms}/dP$ needs to be considered while designing the corrector optics and is pivotal in achieving optimal optical performance over the duration of the entire mission.

Table 4. RMS surface profile deviation induced by 10 Pa change in pressure.

Pressure Change (Pa)	RMS Change in Sag – Fichter (µm)	RMS Change in Sag – FAIM (µm)	RMS Change in Sag – Radar (µm)
480 →490	92.448	92.214	119.704
490→500	91.198	90.890	82.615
500→510	89.990	89.679	98.109
510→520	88.822	88.583	93.088
$\frac{d(Dev)_{rms}}{dP}$	9.06 µm/Pa	9.15 µm/Pa	9.83 µm/Pa

5. Conclusion

The inflatable primary reflector of the OASIS mission brings many opportunities for pioneering science at far lower cost than if more conventional approaches to realizing large space apertures are utilized. To help validate this technical approach, a laser radar system (lidar) is used to measure and confirm the surface profile of a 1 meter inflatable, prototype primary mirror designed using the FAIM modeling program. Experimental measurements are carried out for various operational test cases. The FAIM model was thoroughly checked and cross-verified through two independent methods by comparison with the analytical Fichter model and the experimental lidar measurement data. The predicted shape and measured data were well matched under varying pressures. The presented results successfully verify the high fidelity of FAIM's modeling capability and the utilization of both lidar and deflectometry approaches to performing metrology on large, inflatable, space apertures.

Disclosures. The authors declare no conflicts of interest.

Data availability. Data underlying the results presented in this paper are not publicly available at this time but may be obtained from the authors upon reasonable request

References

1. C. K. Walker, G. Chin, and S. Aalto, *et al.*, "Orbiting Astronomical Satellite for Investigating Stellar Systems (OASIS) Following the Water Trail from the Interstellar Medium to Oceans," Proc. SPIE **11820**, 118200O (2021).
2. M. M. Finckenor and D. Dooling, "Multilayer Insulation Material Guidelines," NASA Tech. Pap., no. April 1999, pp. 1–33, 1999.
3. S. Sirsi, Y. Takashima, A. L. Palisoc, H. Choi, J. W. Arenberg, D. Kim, and C. K. Walker, "Optical Design of the Orbiting Astronomical Satellite for Investigating Stellar Systems (OASIS)," J. Astron. Telesc. Instrum. Syst. **8**(3), 034002 (2022).
4. H. Hencky, "Uber den Spannungszustand in kreisrunden Platten," Z. Math. Phys. **63**, 311–317 (1915).
5. W.B. Fichter, "Some Solutions for the Large Deflections of Uniformly Loaded Circular Membranes," NASA Technical Paper 3658, July 1997.
6. A. L. Palisoc, G. Pardoen, Y. Takashima, A. Chandra, S. Sirsi, H. Choi, D. Kim, H. Quach, J. W. Arenberg, and C. K. Walker, "Analytical and finite element analysis tool for nonlinear membrane antenna modeling for astronomical applications," Proc. SPIE 11820, 118200U (2021).
7. A. B. Meinel and M. P. Meinel, "Inflatable membrane mirrors for optical passband imagery," Opt. Eng. **39**(2), 541–550 (2000).
8. https://www.nikonmetrology.com/en-us/3d-metrology/large-volume-metrology-apdis-mv4×0.
9. H. Quach, H. Kang, S. Sirsi, A. Chandra, H. Choi, M. Esparza, K. Karrfalt, J. Berkson, and Y. Takashima, "Surface Measurement of a Large Inflatable Reflector in Cryogenic Vacuum," Photonics **9**(1), 1 (2022).